Earth and Planetary Science Letters 331–332 (2012) 21–30

Contents lists available at SciVerse ScienceDirect

Earth and Planetary Science Letters

journal homepage: www.elsevier.com/locate/epsl

Quantifying Holocene lithospheric subsidence rates underneath the Mississippi Delta

Shi-Yong Yu [a], Torbjörn E. Törnqvist [a,b,*], Ping Hu [a]

[a] Department of Earth and Environmental Sciences, Tulane University, 6823 St. Charles Avenue, New Orleans, Louisiana 70118-5698, USA
[b] Tulane/Xavier Center for Bioenvironmental Research, Tulane University, 6823 St. Charles Avenue, New Orleans, Louisiana 70118-5698, USA

ARTICLE INFO

Article history:
Received 4 January 2012
Received in revised form 20 February 2012
Accepted 24 February 2012
Available online 30 March 2012

Editor: J. Lynch-Stieglitz

Keywords:
Mississippi Delta
relative sea level
glacial isostatic adjustment
flexural subsidence
Holocene

ABSTRACT

The pattern of Holocene relative sea-level (RSL) change on the US Gulf Coast has been a long-standing subject of debate, featuring opposing scenarios of continuous submergence versus one or more Holocene RSL highstands. The significance of this debate is that the relative role of eustasy, glacial isostatic adjustment (GIA), and lithospheric flexural subsidence associated with Mississippi Delta sediment loading remains unresolved. Here we present a new RSL record from the Louisiana Chenier Plain, >100 km west of the Mississippi Delta margin, based on AMS ^{14}C dated marsh basal peat. This enables us to provide – for the first time – constraints on Holocene lithospheric subsidence rates underneath one of the world's major deltas. Our new record conclusively shows that no middle Holocene RSL highstands occurred on the central US Gulf Coast. Rather, it exhibits a pattern of progressive RSL rise comparable to that from the Mississippi Delta, suggesting that long-wavelength GIA is a dominant deformational process driving lithospheric subsidence in the entire region by means of forebulge collapse. Nevertheless, a 0.15 ± 0.07 mm/yr differential rate of subsidence between the Chenier Plain and key portions of the Mississippi Delta (including the New Orleans metropolitan area) exists. This shows that while the sediment loading effect is real, it is about an order of magnitude smaller than recent studies have postulated.

1. Introduction

Sea-level rise constitutes one of the premier environmental threats of our time, putting coastal and deltaic plains at particular risk given compounding conditions such as low elevations, rapid subsidence rates, and high population densities (Ericson et al., 2006; McGranahan et al., 2007). Nevertheless, surprisingly little is known about lithospheric subsidence rates underneath the world's major depocenters. A comprehensive understanding of mechanisms and rates of deltaic subsidence is critical for the hundreds of millions who inhabit these vulnerable settings.

Quantifying vertical crustal motions in and around large deltaic depocenters relies heavily on the availability of high-resolution relative sea-level (RSL) data over millennial timescales. This is a particularly urgent issue for regions where Holocene RSL reconstructions have led to fundamentally different schools of thought. The US Gulf Coast is one such controversial region where published RSL records derived from different proxies have produced distinctly different interpretations. Specifically, peat-based records exhibit continuous submergence throughout the Holocene at a progressively decreasing rate (Törnqvist et al., 2004a), while records obtained from beach ridges and related phenomena suggest a gradual fall from one or more RSL highstands (up to ~2.5 m above present sea level) during the middle (Blum et al., 2001) and late (Morton et al., 2000) Holocene (Fig. 1A). Resolving this debate is important because it has profound implications for understanding subsidence mechanisms and rates in the Mississippi Delta and its surroundings, a region with some of the highest rates of coastal wetland loss in the world (Day et al., 2007). The RSL highstand scenario would imply that subsidence of the lithosphere underneath the Mississippi Delta is a spatially restricted regional phenomenon, operating at rates of ~1 mm/yr (Blum and Roberts, 2009). In contrast, the continuous submergence scenario has inferred broadly similar RSL histories along the entire US Gulf Coast (Milliken et al., 2008a; Törnqvist et al., 2006), with the implication that lithospheric subsidence rates underneath much of the Mississippi Delta must be about an order of magnitude slower.

The notion of one or more Holocene RSL highstands along the Gulf Coast emerged nearly half a century ago from a study of elevated coastal landforms in the western Gulf of Mexico (Behrens, 1966) and set the stage for a debate that persists today. A review of the history of Holocene sea-level studies along the US Gulf Coast is provided elsewhere (Törnqvist et al., 2004a) and not repeated here. Glacial isostatic adjustment (GIA) models consistently predict that the Gulf Coast exhibits continuous Holocene RSL rise (Milne and Mitrovica, 2008; Peltier, 1996; Simms et al., 2007), representing a characteristic response to high-latitude deglaciation and resulting lithospheric deformation by means of forebulge collapse. Thus, any Holocene RSL highstands would require a re-evaluation of GIA models, with implications well beyond the Gulf of Mexico given model predictions of forebulge collapse extending as far south as northernmost South

* Corresponding author at: Department of Earth and Environmental Sciences, Tulane University, 6823 St. Charles Avenue, New Orleans, Louisiana 70118-5698, USA.
E-mail address: tor@tulane.edu (T.E. Törnqvist).

0012-821X/$ – see front matter © 2012 Elsevier B.V. All rights reserved.
doi:10.1016/j.epsl.2012.02.021

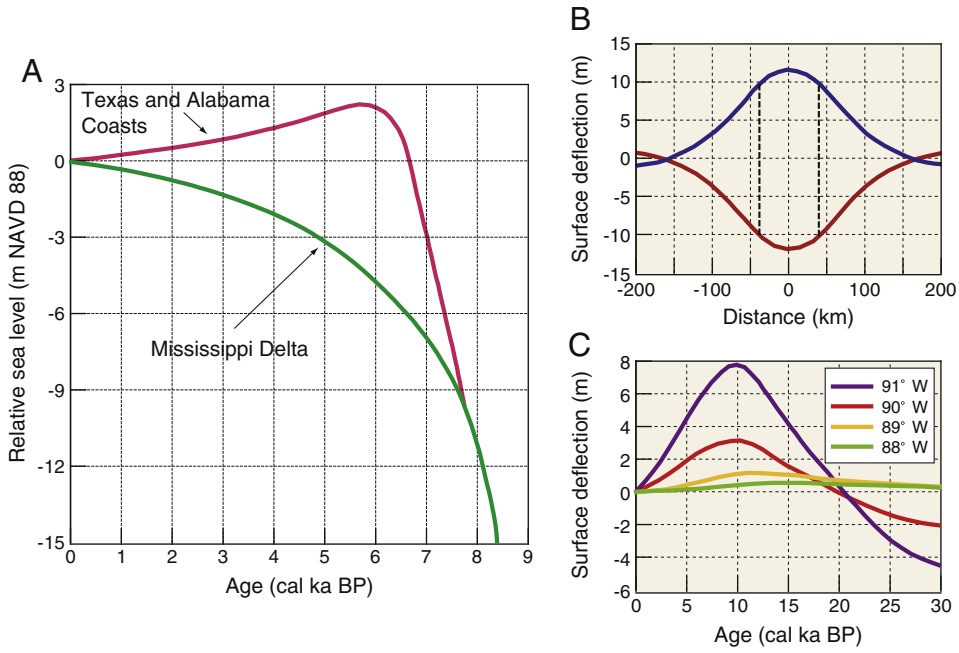

Fig. 1. (A) Contrasting patterns of Holocene RSL change along the US Gulf Coast as obtained from the Mississippi Delta (Törnqvist et al., 2004a) versus the Texas (Blum et al., 2001) and Alabama (Blum et al., 2003) coasts. (B) "Ups and downs" of the Mississippi Delta and its surroundings due to sediment removal and infilling during glacial (blue) and postglacial (red) time, respectively (Blum et al., 2008). Vertical stippled lines indicate position of paleovalley margins. (C) Land-surface deformation at different locations along 30° N during the past 30,000 yrs (Blum et al., 2008). Note that subsidence is predicted at all of these sites during the past 10,000 yrs, albeit at different rates.

America (Milne et al., 2005). It should be noted that these GIA models have to date not incorporated the isostatic effects of deltaic sediment loading.

Based on modeling of the lithospheric flexural deformation (defined here as including both the elastic behavior of the lithosphere and viscous flow in the underlying asthenosphere) driven by sediment unloading and loading in the Mississippi Delta and its underlying paleovalley, Blum et al. (2008) sought to explain the coexistence of a middle Holocene RSL highstand on the Texas (Blum et al., 2001; Morton et al., 2000) and Alabama (Blum et al., 2003) coasts with the continuous submergence reported for the Mississippi Delta. The slower rate of RSL rise in the Mississippi Delta between ~8000 and 6000 cal yr BP (Fig. 1A) would be the result of regional uplift due to unloading associated with valley cutting during the last RSL lowstand (Fig. 1B, C). This large spatial variability in RSL change would imply an important role for lithospheric flexural deformation owing to sediment unloading and loading. A further implication of RSL near or above present during the middle Holocene would be that no significant role could exist in the Gulf of Mexico for the long-wavelength GIA process, and, thus, that the glacial forebulge would be significantly smaller than theoretical studies suggest.

Given that US Gulf Coast RSL records from subsurface peat on one hand and elevated coastal landforms on the other have been obtained from areas that are far apart (Fig. 2A), new and detailed sea-level studies are needed in areas where basal peat and beach ridges coexist. Here we test the hypothesis of Blum et al. (2008) by developing a new, high-resolution RSL record from the Louisiana Chenier Plain. This area is uniquely suited for such a test given that (1) it is located far enough (>100 km) away from the paleovalley margin underneath the Mississippi Delta that the signal of modeled flexural uplift and subsidence should have largely dissipated (Blum et al., 2008) (Fig. 1B); (2) it contains elevated landforms that have been used recently (McBride et al., 2007) to argue for one or more Holocene RSL highstands; and (3) it contains basal peat resting on weathered and consolidated Pleistocene strata (Gould and McFarlan, 1959) that can provide RSL data at a similar resolution as those recently obtained from the Mississippi Delta. Most importantly, such a new record – when compared with recently published RSL records from the Mississippi Delta – could provide an exceptionally accurate and precise estimate of the rate of lithospheric flexural subsidence due to sediment loading. Our study presents the first quantitative constraint on this process underneath one of the Earth's premier depocenters, and offers an approach suitable for application in other world deltas.

2. Materials and methods

2.1. Field sampling

Data collection focused mainly on an area near Little Chenier (Fig. 2B). We restricted our efforts to a relatively small area (~10 km long and 2 km wide) to minimize the potential effects of differential vertical land motions between sampling sites. Boreholes were drilled with an Edelman auger and a hand-operated gouge with a 3 cm diameter, and the cores were described in the field following the US Department of Agriculture texture classification system (Soil Survey Staff, 1999). Once optimal sites for sampling were selected, a ~20-cm-long core segment covering the contact between basal peat and the upper portion of an underlying paleosol was collected (also by hand), using a 6-cm-diameter gouge.

2.2. Differential GPS and optical surveying

To ensure a robust constraint on the elevation of our sea-level index points, extensive optical surveying and differential GPS measurements were carried out. The official benchmark used for elevation control is the National Geodetic Survey (NGS) benchmark AV0426 (29°51′37.5″ N, 93°05′15.7″ W). The orthometric height of this benchmark is 0.65 m relative to the North American Vertical Datum of 1988 (NAVD 88) as reported by NGS in 2004. This benchmark has been designated stability category C, which is defined by NGS as "may hold, but of type commonly subject to surface motion." Six temporary benchmarks close to our sampling sites were set up on the paved road along Little Chenier (Appendix A, Fig. S1). The elevation of these temporary benchmarks relative to AV0426 was determined

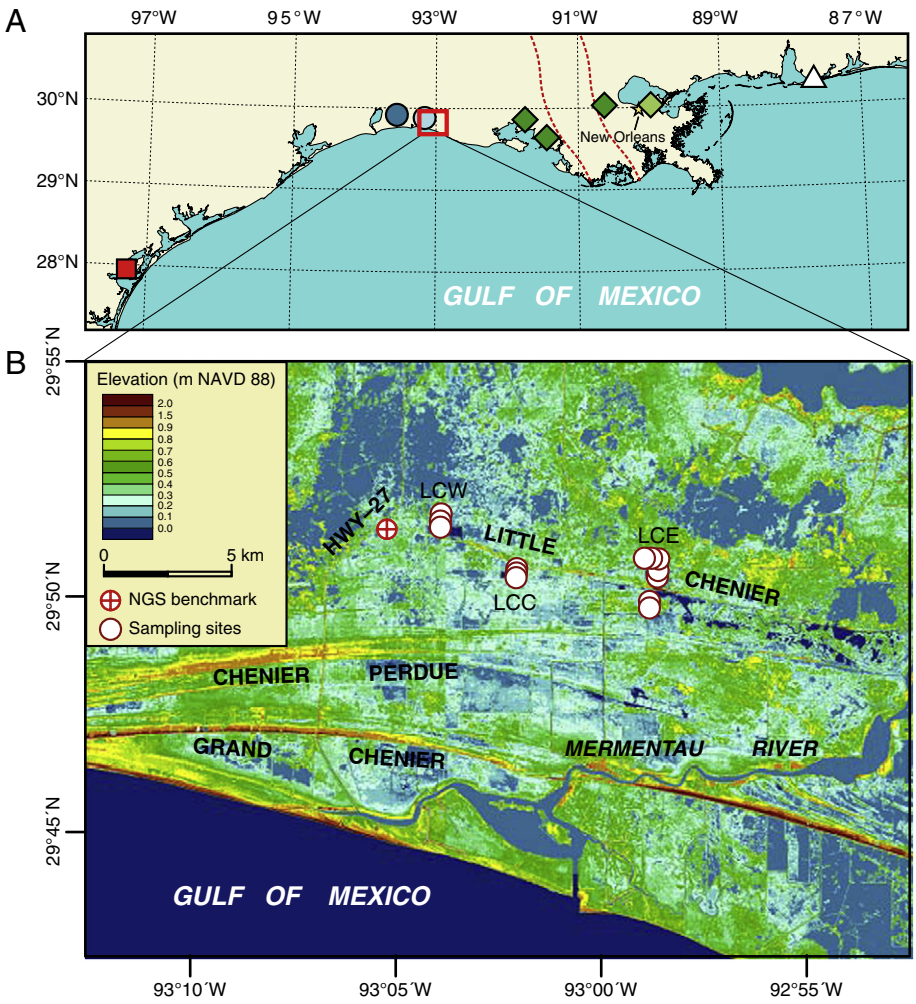

Fig. 2. (A) Overview map with diamonds indicating study areas in the Mississippi Delta where basal peat has revealed a continuous Holocene RSL rise (González and Törnqvist, 2009; Li et al., 2012; Miller, 1983; Törnqvist et al., 2004a, 2004b, 2006). The square and triangle denote study areas on the Texas (Blum et al., 2001) and Alabama (Blum et al., 2003) coast, respectively, where elevated coastal landforms have been used to infer a middle Holocene RSL highstand. Circles indicate previous RSL studies in the Chenier Plain (Gould and McFarlan, 1959; Milliken et al., 2008a) that employed basal peat. Fill colors correspond to RSL data in Fig. 8. Dashed lines indicate margins of the paleovalley underneath the Mississippi Delta during the Last Glacial Maximum. (B) Light Detection and Ranging (LiDAR) image of a portion of the Louisiana Chenier Plain with the three study areas along Little Chenier. LCW = Little Chenier West area; LCC = Little Chenier Central area; LCE = Little Chenier East area.

using a TOPCON GTS-4B electronic total station. Surveying between neighboring temporary benchmarks was repeated at least two times to minimize errors. The surface elevation at the sampling sites was measured with respect to the nearest temporary benchmark at least three times, using the same total station. The elevation of the temporary benchmarks used for sampling was measured independently by means of differential GPS.

The validity of our comparison of RSL records between the Chenier Plain and the Mississippi Delta depends on whether or not differential motions of the benchmarks to which these records were tied have occurred since they were last surveyed by NGS. To verify the elevation difference between AV0426 near Little Chenier and AU3428 (29°48′ 13.6″ N, 91°40′05.9″ W; also stability category C) in the western Mississippi Delta that was used in our previous studies (González and Törnqvist, 2009; Törnqvist et al., 2006), a differential GPS campaign was carried out simultaneously at both benchmarks for about 6 h.

GPS data were processed using the NGS online positioning user service system (http://www.ngs.noaa.gov/OPUS/). Three continuously operating GPS base stations in the region (Houma, LUMCON, and Grand Isle) were included in the solution. The hybrid GEOID03 model (http://www.ngs.noaa.gov/cgi-bin/GEOID_STUFF/geoid03_prompt1.prl) was used for calculating local geoid heights, which were then subtracted from the GPS-derived ellipsoid height to obtain the orthometric height (elevation) of the benchmarks within the NAVD 88 reference framework.

2.3. Stable carbon isotope and organic carbon measurements

Our RSL reconstruction is primarily based on ^{14}C dating of basal peat at different elevations. In a few cases paleosol samples were used. We employ $\delta^{13}C$ measurements of bulk materials to infer the paleosalinity of the wetlands in which these facies accumulated (Chmura et al., 1987). Stable carbon isotope ratios ($\delta^{13}C$) and organic carbon content were measured on both bulk peat and paleosol samples. Samples were first soaked in 10% HCl to remove carbonates, then rinsed repeatedly with deionized water and desiccated thoroughly at 60 °C. The dried samples were homogenized with a pestle and mortar. The measurements were conducted at the Stable Isotope Laboratory, Tulane University, using a Vario MicroCube elemental analyzer connected to an Isoprime isotope ratio monitoring mass spectrometer (irm-MS). Samples were run in triplicate using different sample masses (~0.5, ~1.5, and ~3 mg), and the average of these analyses was calculated and reported with standard deviations reflecting potential heterogeneity of the samples.

2.4. Radiocarbon dating

Our RSL chronology relies primarily on AMS ^{14}C dated plant remains extracted from basal peat. In addition, the paleosol that rests immediately on the largely compaction-free Pleistocene Prairie Complex was used to extend our RSL record. We dated multiple fractions in many of our samples, following an approach similar to previous studies (González and Törnqvist, 2009; Törnqvist et al., 2004a). Slices of 2 to 4 cm in thickness were cut from the very bottom of the basal peat or near the top of the paleosol and sieved with a 250 μm screen to isolate plant remains for dating at the University of California, Irvine. For most samples our dating relies on macrofossils of C_3 plants such as *Scirpus* spp. and *Cladium* spp. In several other cases we dated herbaceous charcoal fragments, preferentially selecting the largest specimens that are least likely to have been transported to the sampling site. For the paleosol samples three separate geochemical fractions (humic acid, residue, and charcoal) were dated. Calibration of ^{14}C ages into calendar years was performed with the OxCal 4.0 program (Bronk Ramsey, 2009).

2.5. Error analysis and sea-level database

Our sea-level index points carry both age and elevation uncertainties arising from a variety of sources. These uncertainties define the error boxes that characterize our RSL records. The age error is defined by the 2σ confidence interval of the calibrated age range. The elevation error is composed of a number of components, including uncertainties associated with non-vertical drilling, sampling, surveying, and the indicative range of the sea-level indicator used. Definitions and in-depth discussion of these sources of error are given elsewhere (Engelhart et al., 2009; Hu, 2010; Shennan, 1982). The total elevation uncertainty, U_{te}, is expressed as

$$U_{te} = T_d + 2 \times E_{te} \quad (1)$$

where T_d is the corrected thickness of the sample to account for compaction which is obtained by multiplying the original sample thickness by 2.5 (Berendsen et al., 2007; Van Asselen, 2011) and E_{te} is the total elevation error which is calculated as

$$E_{te} = \sqrt[2]{E_{ir}^2 + E_s^2 + E_{nv}^2 + E_{lso}^2 + E_{lsg}^2} \quad (2)$$

where:

E_{ir} = indicative range error derived from the difference between mean higher high water (MHHW) and mean tide level (MTL) as measured at eight tide gauges in coastal Louisiana (González and Törnqvist, 2009) (0.15 m);
E_s = sampling error (0.02 m);
E_{nv} = non-vertical drilling error (0.01 × depth (m) below land surface);
E_{lso} = optical surveying error (0.03 m); and
E_{lsg} = GPS surveying error (0.05 m).

An extensive error analysis based on comparable criteria was also conducted for previously published data derived from peat in the same portion of the Chenier Plain (Gould and McFarlan, 1959; Milliken et al., 2008a, 2008b, 2008c) and in the Mississippi Delta (González and Törnqvist, 2009; Li et al., 2012; Miller, 1983; Törnqvist et al., 2004a, 2004b, 2006). In addition, we subjected sea-level data derived from elevated coastal landforms in Texas (Blum et al., 2001) to a similar analysis. We followed a recently established protocol (Hu, 2010) that incorporates a number of sources of error (e.g., uncertainties of ^{14}C ages derived from bulk sediment samples, uncertainties associated with isotopic fractionation correction, correction of sample thickness due to compaction) that have typically not been considered in previous sea-level database studies.

2.6. Regression analysis of RSL records

To enable a quantitative comparison of RSL records from the Chenier Plain and the Mississippi Delta, we carried out a regression analysis using the exponential function

$$RSL(t) = a \times [\exp(\lambda t) - 1] \quad (3)$$

where:

$RSL\ (t)$ = relative sea level as a function of time (m);
a = initial position of relative sea level (m);
t = time (kyr); and
λ = relaxation time (kyr^{-1}).

Curve fitting was conducted by solving a nonlinear optimization problem in a least-squares sense, which was implemented in MATLAB® using the built-in function *lsqnonlin*. For each of the two RSL records, we carried out this regression analysis for the centers of the error boxes and obtained the differential lithospheric motion by subtracting the two curves.

3. Results

3.1. Stratigraphy

The Chenier Plain (Fig. 2B) is a low-lying mudflat interspersed with a series of mostly shore-parallel chenier ridges, the shelly and sandy beach ridges that formed during periods of wave reworking of mudflat deposits (McBride et al., 2007; Russell and Howe, 1935). Stratigraphic investigations based on about 100 hand-drilled boreholes largely confirm findings by previous investigators (Gould and McFarlan, 1959). We selected 13 sites within the Little Chenier area (Fig. 2B) for sampling.

Four distinct stratigraphic units can be recognized in most of the sampled cores (Fig. 3). The basal unit consists of highly consolidated, oxidized, gray-green, silty Pleistocene sediments collectively known as the Prairie Complex (Autin et al., 1991). Blanketing this unit is the weakly developed paleosol mentioned above that consists of a dark gray A-horizon with highly decomposed organic matter. Previous studies (Törnqvist et al., 2004a) have shown that this paleosol reflects the initial stage of organic-matter preservation due to a rising groundwater table that immediately precedes more widespread drowning and peat accumulation. Thus, the paleosol is of a transgressive origin and intimately related with RSL rise, as discussed in more detail later. At most sampling sites the paleosol is onlapped by dark brown peat, which in turn is capped by a light gray mud that largely reflects prograding mudflat deposits. The peat is commonly clayey with herbaceous remains. It is noteworthy that the peat bed is not laterally continuous due to transgressive wave erosion, particularly seaward of Little Chenier (Gould and McFarlan, 1959).

3.2. Elevation analysis

The elevation of six temporary benchmarks used for our sampling was determined by both optical surveying (Appendix A, Table S1) and differential GPS measurements (Appendix A, Table S2). Our results indicate that the differential GPS measurements yield elevations for the temporary benchmarks that corroborate optical surveying within 2 cm. Also, the differential GPS measurements at two NGS benchmarks (i.e., AV0426 near Little Chenier and AU3428 in the western Mississippi Delta) suggest that the elevation difference between these two benchmarks remains valid (Appendix A, Table S3). Thus,

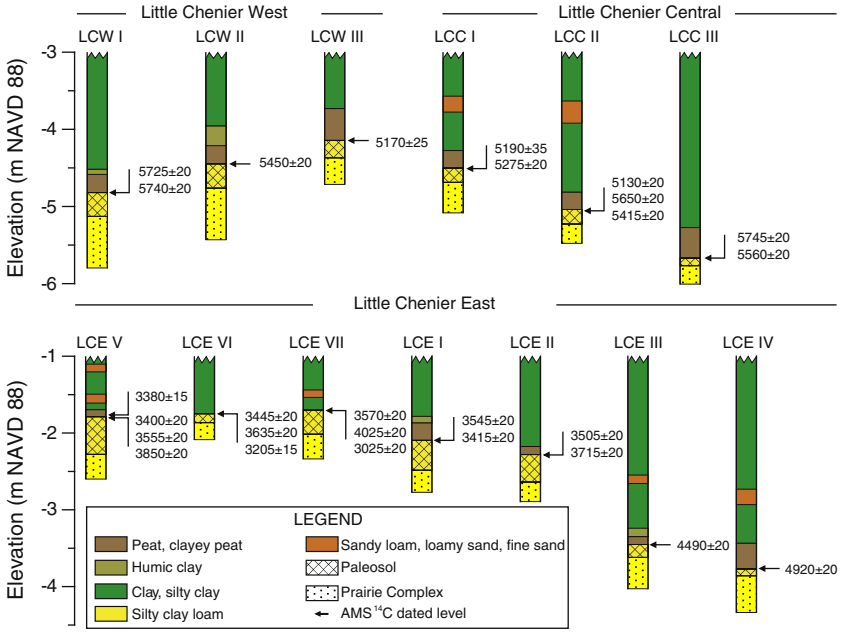

Fig. 3. Stratigraphy of the Pleistocene–Holocene transition zone at sampling sites near Little Chenier. Arrows indicate AMS ^{14}C dated levels. Table 1 provides detailed information about the ^{14}C ages.

we infer that no significant differential subsidence between those two benchmarks has occurred since their elevations were reported.

3.3. Salinity reconstruction

The δ^{13}C data of bulk peat and paleosol samples provide information about the salinity conditions in which these facies accumulated (Appendix A, Table S4). The δ^{13}C value of most of our basal-peat samples varies between −17 and −20‰ (Fig. 4), indicating predominantly brackish conditions within the intertidal zone. The paleosol exhibits δ^{13}C values that are indistinguishable from those for the basal peat (Fig. 4), also reflecting brackish conditions. This confirms that the paleosol formed within the intertidal zone and can be used to obtain sea-level index points. The organic carbon content of basal peat shows large variability, but mostly lies between 3 and 16%. In contrast to the basal peat, the organic carbon content of the paleosol varies between 1 and 3%, which is consistent with the highly decomposed nature of the matrix organic matter.

3.4. Radiocarbon chronology

We obtained 27 AMS ^{14}C ages from different botanical and chemical fractions of the 13 samples; they are shown on the right-hand side of the core logs (Fig. 3). Full documentation of these ^{14}C ages is provided in Table 1. We performed a rigorous geochronological data analysis, including an evaluation of paleosol ^{14}C ages (Fig. 5) that extend our RSL record since the basal peat pinches out at a depth of about −1.7 m (Fig. 3), as well as a careful assessment of basal-peat samples with multiple subsample ^{14}C ages (Fig. 6).

In addition to the δ^{13}C measurements discussed above, the validity of the paleosol as a sea-level indicator is reinforced by its tight temporal relationship with the overlying basal peat. This is illustrated by charcoal extracted from sample Little Chenier East V-2 that yields a ^{14}C age of 3400 ± 20 yr BP, very similar to the age of the overlying basal peat (3380 ± 15 yr BP), also from charcoal (Table 1). Given its fragile nature, charcoal is unlikely to be subject to long-distance transport and thus should represent the true paleosol age. Compared to the charcoal fraction, the ages of humic acid and particularly the residue are systematically older and not in stratigraphic order (Fig. 5) which is likely the result of the presence of reworked, older

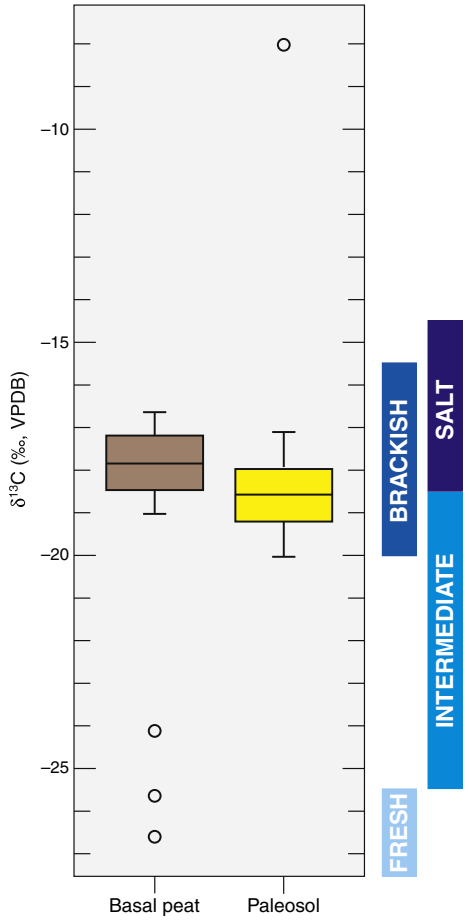

Fig. 4. Comparison of δ^{13}C values for bulk basal peat (N = 24) and paleosol (N = 9) samples with published δ^{13}C ranges from modern sedimentary organic matter in various salinity regimes in coastal Louisiana (Chmura et al., 1987), based on data detailed in Table S4. The horizontal line inside the boxes indicates the mean. The bottom and top sides of the boxes represent the 1σ confidence interval; the bottom and top whiskers represent the 2σ confidence interval. Circles denote outliers that were not included in the calculation of the mean and confidence intervals.

Table 1
^{14}C ages of basal peat and paleosol samples.

Sample name	UTM coordinates (m)[a]		Elevation (m, NAVD 88)	Depth below surface (m)	Material dated	^{14}C age (yr BP)	Laboratory number	Sedimentary facies
	Northing	Easting						
Little Chenier West I-1a	3302.960	493.500	−0.14	4.67–4.70	Charcoal fragments	5725 ± 20	UCIAMS-59680	Basal peat
Little Chenier West I-1b	3302.960	493.500	−0.14	4.67–4.70	Charcoal fragments	5740 ± 20	UCIAMS-59681	Basal peat
Little Chenier West II-1	3303.060	493.540	−0.21	4.24–4.27	*Scirpus* spp. achenes	5450 ± 20	UCIAMS-59682	Basal peat
Little Chenier West III-1	3303.120	493.540	−0.18	3.90–3.93	*Scirpus* spp. achenes	5170 ± 25	UCIAMS-59683	Basal peat
Little Chenier Central I-1a	3301.760	497.160	0.53	4.95–5.01	*Scirpus* spp. achenes	5190 ± 35[b]	UCIAMS-59684	Basal peat
Little Chenier Central I-1b	3301.760	497.160	0.53	4.95–5.01	Charcoal fragments	5275 ± 20[b]	UCIAMS-59685	Basal peat
Little Chenier Central II-1a	3301.680	497.120	0.38	5.22–5.27	*Scirpus* spp. achenes	5130 ± 20[b]	UCIAMS-59686	Basal peat
Little Chenier Central II-1b	3301.680	497.120	0.38	5.22–5.27	*Scirpus* spp. achenes	5650 ± 20[b]	UCIAMS-59687	Basal peat
Little Chenier Central II-1c	3301.680	497.120	0.38	5.22–5.27	Charcoal fragments	5415 ± 20[b]	UCIAMS-66353	Basal peat
Little Chenier Central III-1a	3301.620	497.100	0.17	5.84–5.87	Charcoal fragments	5745 ± 20[b]	UCIAMS-59688	Basal peat
Little Chenier Central III-1b	3301.620	497.100	0.17	5.84–5.87	Charcoal fragments	5560 ± 20[b]	UCIAMS-59689	Basal peat
Little Chenier East I-1a	3301.040	502.060	−0.04	2.11–2.13	*Cladium* spp. seeds	3545 ± 20	UCIAMS-59690	Basal peat
Little Chenier East I-1b	3301.040	502.060	−0.04	2.11–2.13	Charcoal fragments	3415 ± 20	UCIAMS-59691	Basal peat
Little Chenier East II-1a	3300.880	502.040	0.63	2.90–2.92	*Cladium* spp. seeds	3505 ± 20	UCIAMS-59692	Basal peat
Little Chenier East II-1b	3300.880	502.040	0.63	2.90–2.92	Charcoal fragments	3715 ± 20	UCIAMS-59693	Basal peat
Little Chenier East III-1	3300.180	501.740	0.19	3.56–3.60	Charcoal fragments	4490 ± 20	UCIAMS-59694	Basal peat
Little Chenier East IV-1	3299.920	501.740	0.19	3.91–3.93	Charcoal fragments	4920 ± 20	UCIAMS-59695	Basal peat
Little Chenier East V-1	3301.460	502.060	−0.20	1.64–1.67	Charcoal fragments	3380 ± 15	UCIAMS-66354	Basal peat
Little Chenier East V-2a	3301.460	502.060	−0.20	1.69–1.71	Humic acid	3555 ± 20[c]	UCIAMS-66299	Paleosol
Little Chenier East V-2b	3301.460	502.060	−0.20	1.69–1.71	Residue	3850 ± 20[c]	UCIAMS-66298	Paleosol
Little Chenier East V-2c	3301.460	502.060	−0.20	1.69–1.71	Charcoal fragments	3400 ± 20	UCIAMS-66355	Paleosol
Little Chenier East VI-1a	3301.460	501.940	−0.20	1.53–1.56	Humic acid	3445 ± 20[c]	UCIAMS-66301	Paleosol
Little Chenier East VI-1b	3301.460	501.940	−0.20	1.53–1.56	Residue	3635 ± 20[c]	UCIAMS-66300	Paleosol
Little Chenier East VI-1c	3301.460	501.940	−0.20	1.53–1.56	Charcoal fragments	3205 ± 15	UCIAMS-66356	Paleosol
Little Chenier East VII-1a	3301.460	501.840	−0.15	1.55–1.58	Humic acid	3570 ± 20[c]	UCIAMS-66303	Paleosol
Little Chenier East VII-1b	3301.460	501.840	−0.15	1.55–1.58	Residue	4025 ± 20[c]	UCIAMS-66302	Paleosol
Little Chenier East VII-1c	3301.460	501.840	−0.15	1.55–1.58	Charcoal fragments	3025 ± 20	UCIAMS-66357	Paleosol

[a] Zone 15 with reference to NAD 83.
[b] Excluded from sea-level reconstruction (further details provided in text).
[c] Rejected.

organic matter (cf. Schoute, 1984). Therefore, these anomalously old ages were rejected, and wherever paleosol ^{14}C ages factor into our analysis, we picked those based on charcoal. The ^{14}C ages on charcoal reveal the time-transgressive nature of the paleosol: the higher the elevation, the younger the paleosol (Fig. 5). This suggests that the paleosol formed within a relatively short period rather than by means of prolonged pedogenesis, confirming previous inferences (Törnqvist et al., 2004a).

The age of basal-peat subsamples exhibits deviations up to about 500 ^{14}C yrs (Table 1, Fig. 6). Given the high analytical precision of the ^{14}C age measurements, only for those cases where the subsample age difference is less than 50 ^{14}C yrs we calculate a weighted mean. Only sample Little Chenier West I-1 satisfies this requirement, providing a weighted mean age of 5733 ± 14 yr BP. For samples with a larger age deviation (>50 ^{14}C yrs) among subsamples we first note that ^{14}C ages from the Little Chenier Central area show a particularly wide scatter, including a tendency to plot well below data of similar age from the Little Chenier West area (Fig. 6). While some of the anomalously young subsample ages may be the result of bioturbation, this cannot adequately explain the striking offset of Little Chenier Central data. In fact, it may be more conceivable that the older subsample ages were caused by the presence of reworked material.

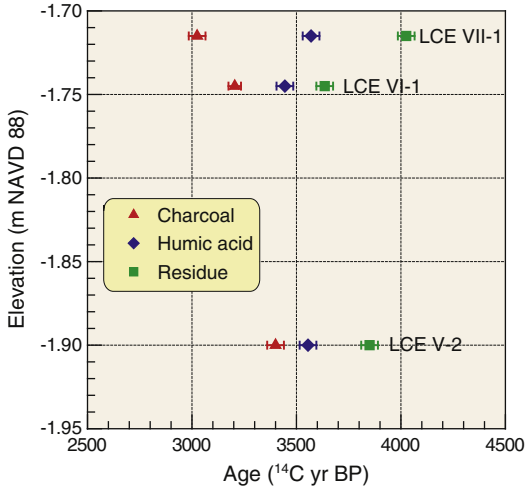

Fig. 5. Comparison of ^{14}C ages with 2σ error bars of different fractions for paleosol samples from the Little Chenier East (LCE) area.

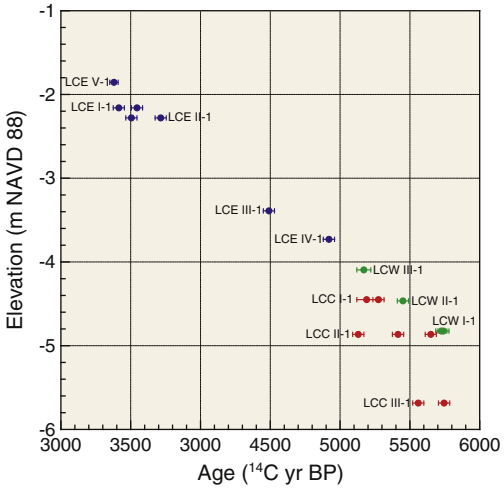

Fig. 6. Comparison of ^{14}C ages with 2σ error bars of different subsamples extracted from basal peat from the Little Chenier West (LCW, green), Little Chenier Central (LCC, red), and Little Chenier East (LCE, blue) areas.

Localized, "hot spot" subsidence and associated wetland loss in coastal Louisiana and Texas have been associated with hydrocarbon production (Kolker et al., 2011; Morton et al., 2006). Fig. 7 shows the spatial distribution, depth, and cumulative production of oil wells in the study area during the past 50 yrs. Sampling sites in the Little Chenier Central area are in close proximity to those oil wells with the highest cumulative production. Therefore, we entertain the possibility that localized, enhanced subsidence may have occurred at these sites due to hydrocarbon withdrawal, but more research is needed to corroborate this. Groundwater withdrawal of sufficient magnitude to substantially enhance subsidence rates occurs preferentially in densely populated areas (Meckel, 2008); our study area belongs to the least populated along the central US Gulf Coast. Given these considerations, we exclude the data from the Little Chenier Central area from our RSL reconstruction and therefore do not include these samples in our subsequent analysis.

We end up with 10 sea-level index points for our RSL reconstruction. In this dataset, samples Little Chenier East I and Little Chenier East II provide subsample ages that differ by 130 and 210 ^{14}C yrs, respectively; too large to justify the use of a weighted mean. In order to choose the most appropriate subsample age from these two samples in an objective manner, we use the sequence option of the OxCal 4.0 calibration program (Bronk Ramsey, 1995) to determine which sequence of 10 stratigraphically constrained ^{14}C ages yields the best consistency as measured by the *A*-index (Appendix A, Fig. S2).

3.5. Relative sea-level record and sea-level database

Given the indicative range (Van de Plassche, 1986) of basal peat and the paleosol (both formed in a brackish environment), the reference water level used in our RSL reconstruction is defined as the average of MHHW and MTL (Engelhart et al., 2009; Shennan, 1982) as obtained from eight tide gauges (González and Törnqvist, 2009). Our new RSL record is presented in Fig. 8. This dataset shows a continuous RSL rise from about –4.8 m at ~6600 cal yr BP to about –1.7 m at ~3200 cal yr BP.

Following the aforementioned protocol, we compiled a regional RSL database that is included as an Excel spreadsheet (Appendix B). This database consists of 85 sea-level index points and 11 limiting data points (all are plotted in Fig. 8). It should be noted that we plot all data with respect to NAVD 88 and use zero elevation as a proxy for present mean sea level. The slight uncertainty associated with this is inconsequential for the purposes of the present study, since our analysis is based entirely on the comparison of sea-level records (rather than to tie these records to present-day tide levels).

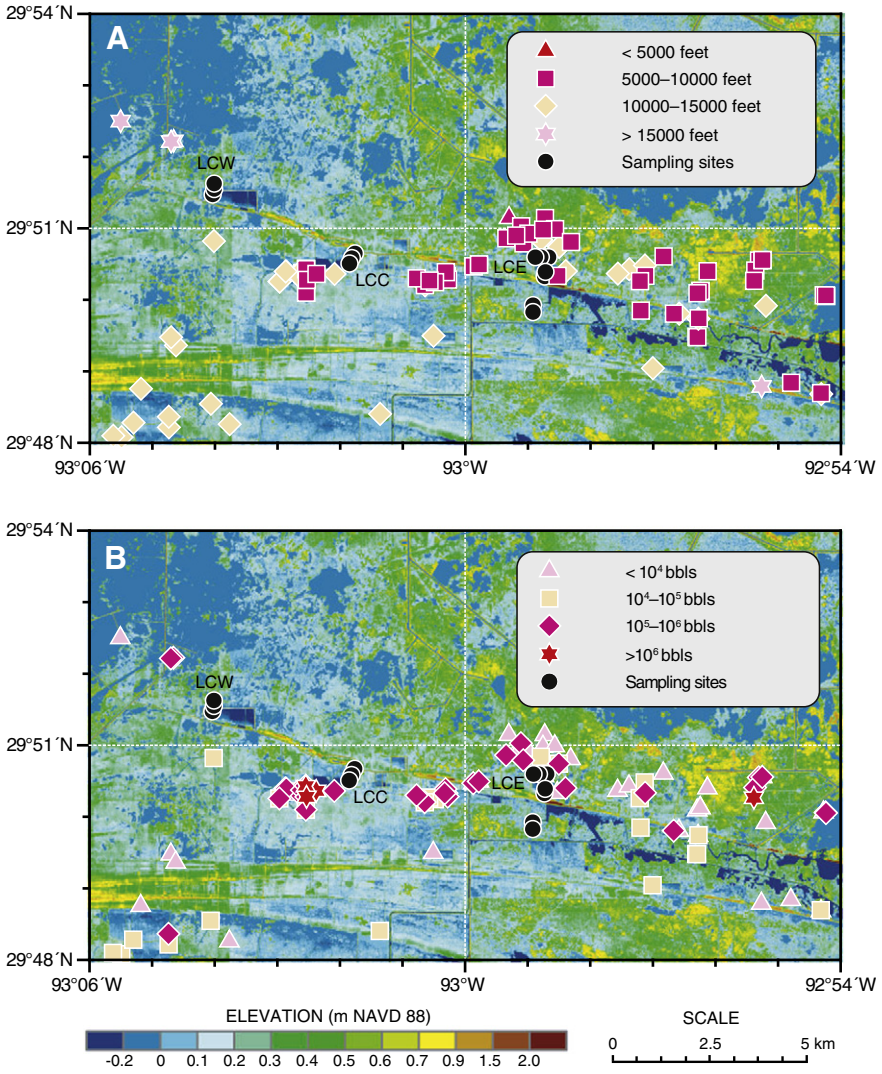

Fig. 7. Maps showing (A) production depth and (B) cumulative production between 1960 and 2010 of oil wells in the study area. 1 ft = 0.3048 m; 1 bbl = 158.987 L. Note that the cumulative production values differ by three orders of magnitude. LCW = Little Chenier West area; LCC = Little Chenier Central area; LCE = Little Chenier East area. For detailed information about the wells, see http://sonris-www.dnr.state.la.us/www_root/sonris_portal_1.htm.

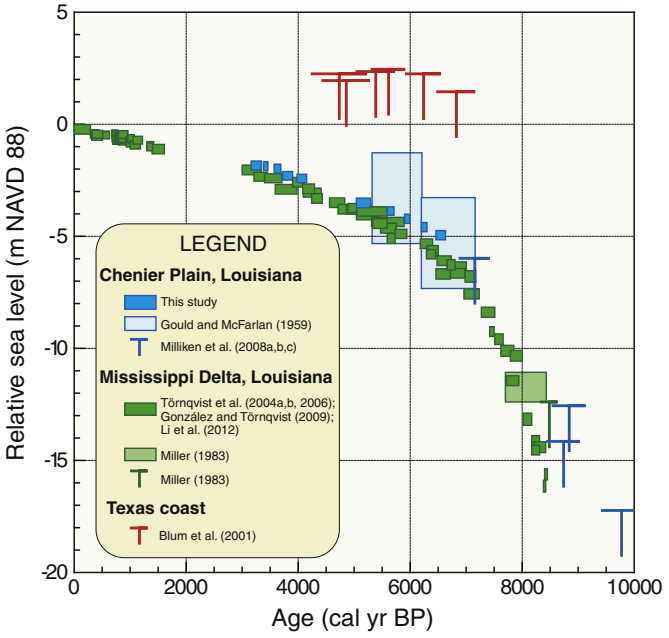

Fig. 8. Comparison of Holocene RSL records derived from basal peat from the Louisiana Chenier Plain (this study, Gould and McFarlan, 1959; Milliken et al., 2008a, 2008b, 2008c) and the Mississippi Delta (González and Törnqvist, 2009; Li et al., 2012; Miller, 1983; Törnqvist et al., 2004a, 2004b, 2006), along with data from elevated coastal landforms from the Texas coast (Blum et al., 2001). Peat-derived data from previous studies (Gould and McFarlan, 1959; Milliken et al., 2008a, 2008b, 2008c) that occur <1 m above a largely compaction-free substrate are also included. A portion of the Chenier Plain RSL data is based on ^{14}C ages of freshwater peat as indicated by δ^{13}C values of –24.5 to –29‰ (Milliken et al., 2008a) and therefore regarded as upper limiting data with mean tide level as the reference water level. The data from Texas are also interpreted as upper limiting data, with mean lower low water as the reference water level given that these landforms and their fossil content have been interpreted as subtidal to intertidal (Blum et al., 2001). For all limiting data, the width of the horizontal bar is defined by the 2σ age error. The length of the vertical bar is arbitrarily defined as 2 m, denoting the uncertainty of their indicative range with respect to mean sea level. Note the large error boxes for the older RSL data from the Chenier Plain (Gould and McFarlan, 1959), owing to sizeable dating and elevation errors. All sea-level index points and limiting data used here, including a full documentation of the relevant variables (nearly 60 in total), are provided in a spreadsheet in Appendix B.

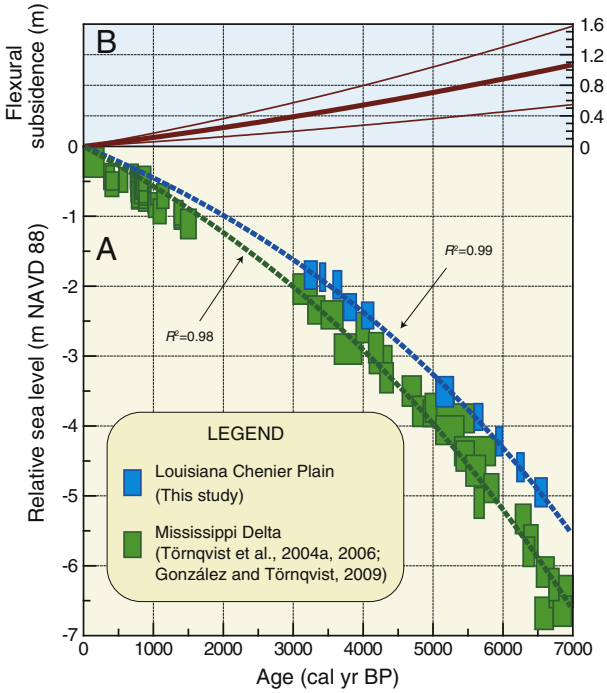

Fig. 9. (A) Comparison of RSL records from the Louisiana Chenier Plain (this study) and the Mississippi Delta (González and Törnqvist, 2009; Törnqvist et al., 2004a, 2006) for the past 7000 yrs. The Mississippi Delta record plots consistently lower than that from the Chenier Plain, revealing lithospheric flexural subsidence due to deltaic sediment loading. Dashed lines are exponential functions fit to the centers of error boxes in these two data sets. (B) The difference between the two regression curves (heavy solid line) defines the lithospheric flexural subsidence of the Pleistocene surface in key portions of the Mississippi Delta during the past 7000 yrs. The error envelope, bounded by two light solid lines denotes the minimum and maximum differential lithospheric motion. The lower bound was obtained by subtracting the regression curve for the upper right corners of the Mississippi Delta RSL record from the lower left corner regression curve for the Chenier Plain RSL record, while the upper bound was obtained by subtracting the regression curve for the lower left corners of the Mississippi Delta RSL record from the upper right corner regression curve for the Chenier Plain RSL record. It should be noted that this is a very conservative approach to assigning an error to our differential subsidence rate; the probability density in the corners of our error boxes is very low given that they are based on 2σ errors, both in the vertical (elevation) and the horizontal (age) direction. Also note that these curves are not entirely linear owing to the subtraction of two exponential curves; this does not necessarily imply that the flexure rate decreased with time.

4. Discussion

Our new sea-level index points from the Chenier Plain plot up to 5 to 7 m below coeval RSL data inferred from elevated coastal landforms in Texas (Fig. 8). As discussed above, we have considered several chronological models for our RSL record. However, it is important to note that no matter which chronological model is used, our data always plot far below the presumed middle Holocene RSL highstand. Thus, our findings are robust.

We conducted a similar rigorous error analysis of previously published RSL data derived from basal peat in this region (Gould and McFarlan, 1959; Milliken et al., 2008a, 2008b, 2008c). Our RSL record is consistent with these data (Fig. 8). Taken together, the RSL record from the Chenier Plain exhibits a progressive rise, comparable to that revealed by our RSL data from the Mississippi Delta (González and Törnqvist, 2009; Li et al., 2012; Törnqvist et al., 2004a, 2004b, 2006). Although our new data only cover the middle Holocene, the broad similarity with the Mississippi Delta record suggests that continuous RSL rise that prevailed there throughout the late Holocene should be expected in the Chenier Plain as well. The up to 3 m high Little Chenier has been dated to 2775 ^{14}C yr BP (Gould and McFarlan, 1959) which corresponds to ~2900 cal yr BP, thus postdating our youngest sea-level index point (Fig. 8) only by a small margin. If Little Chenier would represent a late Holocene RSL highstand as has been postulated (McBride et al., 2007), a dramatic sea-level rise of several meters would have occurred within ~300 yrs, a scenario that we dismiss given the absence of evidence for this from high-resolution RSL records worldwide.

The broad similarity between the Chenier Plain and the Mississippi Delta RSL records implies a common forcing mechanism. As the eustatic contribution was strongly reduced after ~7000 cal yr BP (Fleming et al., 1998), the continued submergence in these two areas was mainly an expression of subsidence of Pleistocene and underlying strata. This was predominantly caused by the continental-scale GIA process associated with deglaciation in high-latitude North America, which drives land subsidence along the US Gulf Coast by means of forebulge collapse.

Despite these broad similarities, the Chenier Plain RSL data plot systematically higher than those from the Mississippi Delta (Fig. 8). Closer inspection reveals that this is particularly the case for the oldest portion of the Chenier Plain record, a trend that is consistent with the fact that older limiting RSL data from this region (Milliken et al., 2008a, 2008b, 2008c) typically plot several meters above Mississippi Delta RSL data of similar age. Given the orientation of the region relative to the former margin of the Laurentide Ice Sheet, differential GIA (including ocean loading) effects are unlikely. According to our GPS measurements (Appendix A, Table S3), the difference between RSL

data from the Chenier Plain and the Mississippi Delta cannot be attributed to differential vertical motion of benchmarks. Therefore, the observed divergence of the two records, going back in time, must be a manifestation of lithospheric flexural subsidence underneath the Mississippi Delta associated with deltaic sediment loading.

The paired RSL records from the Chenier Plain and the Mississippi Delta for the past 7000 yrs (Fig. 9A) enable us to quantify the rate of lithospheric flexural subsidence due to the sediment loading effect in those portions of the Mississippi Delta from where our RSL records were obtained. Our regression analysis reveals a differential subsidence between the Chenier Plain and the Mississippi Delta of 1.05 ± 0.50 m during this time period (Fig. 9B), equivalent to an average rate of 0.15 ± 0.07 mm/yr. This rate is similar to that derived from biostratigraphic data in the New Orleans metropolitan area dating back to the middle Miocene (Edrington et al., 2008) and only slightly smaller than a rate for the past ~10 myrs (0.26 mm/yr), obtained about 100 km southeast of New Orleans (Straub et al., 2009). It is well established (Fisk and McFarlan, 1955) that the elevation of the deformed surface of the Prairie Complex underneath the Mississippi Delta can be used as a proxy for subsidence, with a distinct pattern of rapidly increasing subsidence rates in a seaward direction. Contour lines of the Prairie Complex surface in our study areas in the Mississippi Delta extend through the New Orleans metropolitan area (Fisk and McFarlan, 1955; Saucier, 1994). Indeed, a sea-level index point from basal peat within this area (Miller, 1983) plots at a similar elevation as RSL data from other portions of the delta (Fig. 8), indicating subsidence rates of a comparable magnitude. These results show that the rates of RSL rise of ~10 mm/yr as observed for the past century in the Mississippi Delta (Penland and Ramsey, 1990) must primarily be the result of processes within the Holocene succession, notably sediment compaction (Törnqvist et al., 2008).

While our findings confirm that the deltaic sediment loading effect does cause spatial variability of Holocene RSL change as advocated by Blum et al. (2008), their model overpredicts the magnitude of flexural vertical motion. We note that the rapid divergence between ~8000 and 6000 cal yr BP between the basal peat and beach ridge RSL data (Fig. 1A) was explained (Blum et al., 2008) as the result of uplift in and near the Mississippi Delta resulting from sediment unloading due to valley cutting (Fig. 1B). However, their reconstructions show that the majority of sediment excavation and resulting valley-margin uplift occurred between 30,000 and 15,000 cal yr BP (Fig. 1 C), i.e., long before the inferred RSL response.

The newly obtained rate of flexural subsidence in the Mississippi Delta enables us to evaluate the average late Holocene GIA rate along the central US Gulf Coast. However, it must be stressed that this analysis is tentative and will require GIA modeling to address, among others, the role of rotational and gravitational effects on the geoid in the Gulf of Mexico during the late Holocene (cf. Shennan et al., 2012). Given that the background rate of RSL rise in the Mississippi Delta during the pre-industrial millennium is ~0.6 mm/yr (González and Törnqvist, 2009) and assuming that the late Holocene eustatic component is close to zero (Lambeck et al., 2004; but see Gehrels (2010) for a critical evaluation), subtracting the flexural component (i.e., ~0.15 mm/yr) yields a value of ~0.45 mm/yr. We first note that this value likely includes some long-term passive margin subsidence. On the other hand, a contribution of ocean siphoning (Mitrovica and Milne, 2002; Mitrovica and Peltier, 1991), estimated at ~0.3 mm/yr of sea-level fall (Gehrels, 2010; Jansen et al., 2007), could potentially increase our inferred value. We note, however, that the estimated rate of ~0.45 mm/yr is similar to a recently obtained value for forebulge collapse in South Carolina (Engelhart et al., 2009) which is located at an equal distance from the center of glaciation in the western Hudson Bay area. Compared with the GIA component, the sediment-loading effect plays a smaller role, at least in landward portions of the Mississippi Delta, and it is at least an order of magnitude smaller than what recent model studies have suggested (Blum et al., 2008; Hutton and Syvitski, 2008; Ivins et al., 2007).

Our new findings also allow us to address the issue of 20th century acceleration of RSL rise on the central US Gulf Coast, outside of the Mississippi Delta. The best available tide-gauge record is at Pensacola, Florida, given its length (>80 yrs) and its location on tectonically relatively stable Pliocene strata. Indeed, the long-term trend of ~2.1 mm/yr (González and Törnqvist, 2006; Kolker et al., 2011) at this site is among the lowest on the central US Gulf Coast. Given the pre-industrial rate of GIA-dominated RSL rise for this region of ~0.45 mm/yr, we observe a nearly fivefold acceleration that echoes the marked sea-level acceleration seen worldwide (Gehrels, 2010). We note that correcting the Pensacola tide-gauge record for our tentative GIA rate yields a value of ~1.65 mm/yr, similar to the globally averaged rate of eustatic sea-level rise for the past century (Church and White, 2006).

Finally, our new findings show that the elevated beach ridges that occur along significant portions of the US Gulf Coast require reinterpretation. A storm origin has been discarded in the past (Morton et al., 2000) based on the argument that tropical cyclones tend to be destructive rather than constructive and typically flatten any near-shore topography (at least in the spatially restricted areas subject to direct hurricane strikes). Storm surges submerge elevated landforms farther inland that tend to be morphologically unaffected. However, a recent hypothesis (Donnelly and Giosan, 2008) postulates that elevated beach ridges might be the result not of direct tropical cyclone impacts, but rather the swell associated with prolonged periods of higher storm activity within the wider Gulf of Mexico (i.e., a much larger region than that directly affected by storms during landfall). A proxy record of Holocene wind strength from a Texas estuary (Troiani et al., 2011) lends tentative support to the notion of increased wind activity during the middle Holocene. Further examination of these ideas is warranted and will require detailed monitoring of present-day shoreline morphodynamics associated with storm activity. As a final note, targeted and quantitative studies of the indicative meaning and indicative range of sea-level indicators derived from beach-ridge facies in this region, similar to what has been done elsewhere (Roep and Beets, 1988), should be welcomed.

5. Conclusions

A new, high-resolution middle Holocene RSL record from the Louisiana Chenier Plain bears an overall striking resemblance to recently published RSL data from the Mississippi Delta. Collectively, they exhibit continuous submergence of the central US Gulf Coast during the past 7000 yrs, providing conclusive evidence against the presence of Holocene RSL highstands in this region. This similarity suggests that continental-scale GIA associated with deglaciation in high-latitude North America is a dominant deformational process that drives subsidence of the Pleistocene basement on the central US Gulf Coast. Nevertheless, a subtle difference between Holocene RSL records from the Chenier Plain and the Mississippi Delta reveals a deltaic sediment loading effect, which is estimated to be 0.15 ± 0.07 mm/yr in those portions of the delta that harbor the largest populations. Therefore, lithospheric flexural subsidence due to this effect is less prominent than GIA, and up to several orders of magnitude smaller than shallow subsidence processes (compaction) in the Holocene column. Our findings constitute the first study that quantifies millennial-scale lithospheric subsidence rates underneath one of the world's largest depocenters, and offers considerable scope for similar analyses in other major deltas.

Supplementary data related to this article can be found online at doi:10.1016/j.epsl.2012.02.021.

Acknowledgments

Support for this work was provided by the US National Science Foundation (BCS-0519764 and EAR-0719179), along with NOAA and USGS through the Long-term Estuary Assessment Group (LEAG) program and Tulane's Research Enhancement Fund. We thank M.J. Blum and C.J. Saunders for their kind help with identifying plant macrofossils and B. Kohl for pointing us to hydrocarbon extraction records. Our gratitude is also extended to the Rockefeller Wildlife Refuge for logistical assistance and to landowners in Cameron Parish for allowing us access to their property. We are grateful to UNAVCO, Inc., for technical support during the GPS campaign and to J. Southon and his staff for ^{14}C dating. We acknowledge J.A. Menking, Y.-X. Li, Z.-X. Shen, J.L. González, J.I. Kuykendall, and B.E. Rosenheim for assistance during field and laboratory work. M.D. Blum provided perceptive comments on an earlier draft, but we stress that the interpretations presented herein are our own. Thoughtful reviews were provided by W.R Gehrels and an anonymous referee.

References

Autin, W.J., Burns, S.F., Miller, B.J., Saucier, R.T., Snead, J.I., 1991. Quaternary geology of the Lower Mississippi Valley. In: Morrison, R.B. (Ed.), Quaternary Nonglacial Geology: Conterminous U.S. Geological Society of America, Boulder, pp. 547–582.

Behrens, E.W., 1966. Recent emerged beach in eastern Mexico. Science 152, 642–643.

Berendsen, H.J.A., et al., 2007. New groundwater-level rise data from the Rhine-Meuse delta — implications for the reconstruction of Holocene relative mean sea-level rise and differential land-level movements. Neth. J. Geosci. — Geol. Mijnbouw 86, 333–354.

Blum, M.D., et al., 2001. Middle Holocene sea-level rise and highstand at +2 m, central Texas Coast. J. Sediment. Res. 71, 581–588.

Blum, M.D., Roberts, H.H., 2009. Drowning of the Mississippi Delta due to insufficient sediment supply and global sea-level rise. Nat. Geosci. 2, 488–491.

Blum, M.D., Sivers, A.E., Zayac, T., Goble, R.J., 2003. Middle Holocene sea-level and evolution of the Gulf of Mexico coast. Gulf Coast Assoc. Geol. Soc. Trans. 53, 64–77.

Blum, M.D., Tomkin, J.H., Purcell, A., Lancaster, R.R., 2008. Ups and downs of the Mississippi Delta. Geology 36, 675–678.

Bronk Ramsey, C., 1995. Radiocarbon calibration and analysis of stratigraphy: the OxCal program. Radiocarbon 37, 425–430.

Bronk Ramsey, C., 2009. Bayesian analysis of radiocarbon dates. Radiocarbon 51, 337–360.

Chmura, G.L., Aharon, P., Socki, R.A., Abernethy, R., 1987. An inventory of ^{13}C abundances in coastal wetlands of Louisiana, USA: vegetation and sediments. Oecologia 74, 264–271.

Church, J.A., White, N.J., 2006. A 20th century acceleration in global sea-level rise. Geophys. Res. Lett. 33, L01602.

Day Jr., J.W., et al., 2007. Restoration of the Mississippi Delta: lessons from Hurricanes Katrina and Rita. Science 315, 1679–1684.

Donnelly, J.P., Giosan, L., 2008. Tempestuous highs and lows in the Gulf of Mexico. Geology 36, 751–752.

Edrington, C.H., Blum, M.D., Nunn, J.A., Hanor, J.S., 2008. Long-term subsidence and compaction rates: a new model for the Michoud area, south Louisiana. Gulf Coast Assoc. Geol. Soc. Trans. 58, 261–272.

Engelhart, S.E., Horton, B.P., Douglas, B.C., Peltier, W.R., Törnqvist, T.E., 2009. Spatial variability of late Holocene and 20th century sea-level rise along the Atlantic coast of the United States. Geology 37, 1115–1118.

Ericson, J.P., Vörösmarty, C.J., Dingman, S.L., Ward, L.G., Meybeck, M., 2006. Effective sea-level rise and deltas: causes of change and human dimension implications. Global Planet. Change 50, 63–82.

Fisk, H.N., McFarlan Jr., E., 1955. Late Quaternary deltaic deposits of the Mississippi River. Geol. Soc. Am. Spec. Pap. 62, 279–302.

Fleming, K., et al., 1998. Refining the eustatic sea-level curve since the Last Glacial Maximum using far- and intermediate-field sites. Earth Planet. Sci. Lett. 163, 327–342.

Gehrels, R., 2010. Sea-level changes since the Last Glacial Maximum: an appraisal of the IPCC Fourth Assessment Report. J. Quat. Sci. 25, 26–38.

González, J.L., Törnqvist, T.E., 2006. Coastal Louisiana in crisis: subsidence or sea level rise? Eos 87, 493–498.

González, J.L., Törnqvist, T.E., 2009. A new Late Holocene sea-level record from the Mississippi Delta: evidence for a climate/sea level connection? Quat. Sci. Rev. 28, 1737–1749.

Gould, H.R., McFarlan Jr., E., 1959. Geologic history of the chenier plain, southwestern Louisiana. Gulf Coast Assoc. Geol. Soc. Trans. 9, 261–270.

Hu, P., 2010. Developing a quality-controlled postglacial sea-level database for coastal Louisiana to assess conflicting hypotheses of Gulf Coast sea-level change. MS thesis, Tulane University.

Hutton, E.W.H., Syvitski, J.P.M., 2008. Sedflux 2.0: an advanced process-response model that generates three-dimensional stratigraphy. Comput. Geosci. 34, 1319–1337.

Ivins, E.R., Dokka, R.K., Blom, R.G., 2007. Post-glacial sediment load and subsidence in coastal Louisiana. Geophys. Res. Lett. 34, L16303.

Jansen, E., et al., 2007. Palaeoclimate. In: Solomon, S., Qin, D., Manning, M., Chen, Z., Marquis, M., Averyt, K.B., Tignor, M., Miller, H.L. (Eds.), Climate Change 2007. The Physical Science Basis. Cambridge University Press, Cambridge, pp. 433–497.

Kolker, A.S., Allison, M.A., Hameed, S., 2011. An evaluation of subsidence rates and sea-level variability in the northern Gulf of Mexico. Geophys. Res. Lett. 38, L21404.

Lambeck, K., Anzidei, M., Antonioli, F., Benini, A., Esposito, A., 2004. Sea level in Roman time in the Central Mediterranean and implications for recent change. Earth Planet. Sci. Lett. 224, 563–575.

Li, Y.-X., Törnqvist, T.E., Nevitt, J.M., Kohl, B., 2012. Synchronizing a sea-level jump, final Lake Agassiz drainage, and abrupt cooling 8200 years ago. Earth Planet. Sci. Lett. 315–316, 41–50.

McBride, R.A., Taylor, M.J., Byrnes, M.R., 2007. Coastal morphodynamics and Chenier-Plain evolution in southwestern Louisiana, USA: a geomorphic model. Geomorphology 88, 367–422.

McGranahan, G., Balk, D., Anderson, B., 2007. The rising tide: assessing the risks of climate change and human settlements in low elevation coastal zones. Environ. Urban. 19, 17–37.

Meckel, T.A., 2008. An attempt to reconcile subsidence rates determined from various techniques in southern Louisiana. Quat. Sci. Rev. 27, 1517–1522.

Miller III, W., 1983. Stratigraphy of newly exposed Quaternary sediments, eastern Orleans Parish, Louisiana. Tulane Stud. Geol. Paleontol. 17, 85–104.

Milliken, K.T., Anderson, J.B., Rodriguez, A.B., 2008a. A new composite Holocene sea-level curve for the northern Gulf of Mexico. Geol. Soc. Am. Spec. Pap. 443, 1–11.

Milliken, K.T., Anderson, J.B., Rodriguez, A.B., 2008b. Record of dramatic Holocene environmental changes linked to eustasy and climate change in Calcasieu Lake, Louisiana, USA. Geol. Soc. Am. Spec. Pap. 443, 43–63.

Milliken, K.T., Anderson, J.B., Rodriguez, A.B., 2008c. Tracking the Holocene evolution of Sabine Lake through the interplay of eustasy, antecedent topography, and sediment supply variations, Texas and Louisiana, USA. Geol. Soc. Am. Spec. Pap. 443, 65–88.

Milne, G.A., Long, A.J., Bassett, S.E., 2005. Modelling Holocene relative sea-level observations from the Caribbean and South America. Quat. Sci. Rev. 24, 1183–1202.

Milne, G.A., Mitrovica, J.X., 2008. Searching for eustasy in deglacial sea-level histories. Quat. Sci. Rev. 27, 2292–2302.

Mitrovica, J.X., Milne, G.A., 2002. On the origin of late Holocene sea-level highstands within equatorial ocean basins. Quat. Sci. Rev. 21, 2179–2190.

Mitrovica, J.X., Peltier, W.R., 1991. On postglacial geoid subsidence over the equatorial oceans. J. Geophys. Res. 96, 20053–20071.

Morton, R.A., Bernier, J.C., Barras, J.A., 2006. Evidence of regional subsidence and associated interior wetland loss induced by hydrocarbon production, Gulf Coast region, USA. Environ. Geol. 50, 261–274.

Morton, R.A., Paine, J.G., Blum, M.D., 2000. Responses of stable bay-margin and barrier-island systems to Holocene sea-level highstands, western Gulf of Mexico. J. Sediment. Res. 70, 478–490.

Peltier, W.R., 1996. Mantle viscosity and ice-age ice sheet topography. Science 273, 1359–1364.

Penland, S., Ramsey, K.E., 1990. Relative sea-level rise in Louisiana and the Gulf of Mexico: 1908–1988. J. Coast. Res. 6, 323–342.

Roep, T.B., Beets, D.J., 1988. Sea level rise and paleotidal levels from sedimentary structures in the coastal barriers in the western Netherlands since 5600 BP. Geol. Mijnbouw 67, 53–60.

Russell, R.J., Howe, H.V., 1935. Cheniers of southwestern Louisiana. Geogr. Rev. 25, 449–461.

Saucier, R.T., 1994. Geomorphology and Quaternary Geologic History of the Lower Mississippi Valley. Mississippi River Commission, Vicksburg.

Schoute, J.F.Th., 1984. Vegetation horizons and related phenomena. A palaeoecological–micromorphological study in the younger coastal Holocene of the northern Netherlands (Schildmeer area). Dissert. Botanicæ 81, 1–270.

Shennan, I., 1982. Interpretation of Flandrian sea-level data from the Fenland, England. Proc. Geol. Assoc. 93, 53–63.

Shennan, I., Milne, G., Bradley, S., 2012. Late Holocene vertical land motion and relative sea-level changes: lessons from the British Isles. J. Quat. Sci. 27, 64–70.

Simms, A.R., Lambeck, K., Purcell, A., Anderson, J.B., Rodriguez, A.B., 2007. Sea-level history of the Gulf of Mexico since the Last Glacial Maximum with implications for the melting history of the Laurentide Ice Sheet. Quat. Sci. Rev. 26, 920–940.

Soil Survey Staff, 1999. Soil Taxonomy. A Basic System of Soil Classification for Making and Interpreting Soil Surveys. United States Department of Agriculture, Washington.

Straub, K.M., Paola, C., Mohrig, D., Wolinsky, M.A., George, T., 2009. Compensational stacking of channelized sedimentary deposits. J. Sediment. Res. 79, 673–688.

Törnqvist, T.E., Bick, S.J., González, J.L., Van der Borg, K., De Jong, A.F.M., 2004b. Tracking the sea-level signature of the 8.2 ka cooling event: new constraints from the Mississippi Delta. Geophys. Res. Lett. 31, L23309.

Törnqvist, T.E., Bick, S.J., Van der Borg, K., De Jong, A.F.M., 2006. How stable is the Mississippi Delta? Geology 34, 697–700.

Törnqvist, T.E., et al., 2004a. Deciphering Holocene sea-level history on the U.S. Gulf Coast: a high-resolution record from the Mississippi Delta. Geol. Soc. Am. Bull. 116, 1026–1039.

Törnqvist, T.E., et al., 2008. Mississippi Delta subsidence primarily caused by compaction of Holocene strata. Nat. Geosci. 1, 173–176.

Troiani, B.T., Simms, A.R., Dellapenna, T., Piper, E., Yokoyama, Y., 2011. The importance of sea-level and climate change, including changing wind energy, on the evolution of a coastal estuary: Copano Bay, Texas. Mar. Geol. 280, 1–19.

Van Asselen, S., 2011. The contribution of peat compaction to total basin subsidence: implications for the provision of accommodation space in organic-rich deltas. Basin Res. 23, 239–255.

Van de Plassche, O., 1986. Introduction. In: Van de Plassche, O. (Ed.), Sea-Level Research: a Manual for the Collection and Evaluation of Data. Geo Books, Norwich, pp. 1–26.